A Role for the Serine/Arginine-Rich (SR) Protein B52/SRSF6 in Cell Growth and Myc Expression in *Drosophila*

Céline Fernando,*,†,1 Agnès Audibert,§,1 Françoise Simon,§ Jamal Tazi,*,†,2 and François Juge*,†,2

*Institut de Génétique Moléculaire de Montpellier, Unité Mixte de Recherche 5535, Centre National de la Recherche Scientifique, 1919 route de Mende, 34293 Montpellier Cedex 5, France, †Université de Montpellier, 163 rue Auguste Broussonnet, 34090 Montpellier, France, and §Sorbonne Universités, Université Pierre et Marie Curie Paris 06, Centre National de la Recherche Scientifique Unité Mixte de Recherche 7622, Laboratoire de Biologie du Développement, F-75005, Paris, France

ABSTRACT Serine-/arginine-rich (SR) proteins are RNA-binding proteins that are primarily involved in alternative splicing. Expression of some SR proteins is frequently upregulated in tumors, and previous reports have demonstrated that these proteins can directly participate in cell transformation. Identifying factors that can rescue the effects of SR overexpression *in vivo* is, therefore, of potential therapeutic interest. Here, we analyzed phenotypes induced by overexpression of the SR protein B52 during *Drosophila* development and identified several proteins that can rescue these phenotypes. Using the mechanosensory bristle lineage as a developmental model, we show that B52 expression level influences cell growth, but not differentiation, in this lineage. In particular, B52 overexpression increases cell growth, upregulates *myc* transcription, and gives rise to flies lacking thoracic bristles. Using a genetic screen, we identified several suppressors of the phenotypes induced by overexpression of B52 *in vivo* in two different organs. We show that upregulation of *brain tumor* (*brat*), a tumor suppressor and post-transcriptional repressor of *myc*, and downregulation of *lilliputian* (*lilli*), a subunit of the superelongation complex involved in transcription elongation, efficiently rescue the phenotypes induced by B52 overexpression. Our results demonstrate a role of this SR protein in cell growth and identify candidate proteins that may overcome the effects of SR protein overexpression in mammals.

KEYWORDS SR protein; cell growth; Myc; genetic screen

SERINE-/arginine-rich (SR) proteins form a conserved family of RNA-binding proteins that play crucial roles in the control of gene expression. These proteins were first characterized as pre-mRNA splicing factors involved in both constitutive and alternative RNA splicing (Lin and Fu 2007). They particularly act as concentration-dependent modulators of alternative RNA splicing, often in competition with other RNA-binding proteins, such as hnRNPs (Chen and Manley 2009). In addition to this well-characterized role in RNA splicing, several SR proteins participate in other steps of RNA metabolism, including transcription elongation, RNA export, decay, and translation (Zhong *et al.* 2009). By integrating these functions, SR proteins may facilitate coordination between different steps of mRNA metabolism to precisely control gene expression and maintain cellular homeostasis. Several mechanisms controlling either the level or the activity of SR proteins have been identified. Post-translational modifications of the RS domain of SR proteins modulates SR protein activity and distribution in the cell (Zhou and Fu 2013), whereas the level of SR proteins can be controlled by autoregulation (Sun *et al.* 2010), by microRNA-based translational repression (Wu *et al.* 2010), and through tethering by long noncoding RNA (Tripathi *et al.* 2010).

The importance of regulating SR protein activity is particularly illustrated by the effects of SR protein overexpression in mammalian cells and *Drosophila*. In mammals, overexpression of SRSF1 and SRSF6 results in immortalization of cells that form tumors in mice (Karni *et al.* 2007; Cohen-Eliav *et al.* 2013). Moreover, the expression of these SR proteins is frequently upregulated in several tumor types, suggesting that the proteins contribute to tumor emergence and/or growth.

doi: 10.1534/genetics.115.174391
Manuscript received January 9, 2015; accepted for publication February 11, 2015; published Early Online February 12, 2015.
Available freely online through the author-supported open access option.
Supporting information is available online at http://www.genetics.org/lookup/suppl/doi:10.1534/genetics.115.174391/-/DC1.
[1]These authors contributed equally to this work.
[2]Corresponding authors: Institut de Génétique Moléculaire de Montpellier, CNRS UMR5535, 1919 route de Mende, 34293 Montpellier Cedex 5, France.
E-mail: francois.juge@igmm.cnrs.fr; jamal.tazi@igmm.cnrs.fr

In *Drosophila*, targeted overexpression of most SR proteins during eye differentiation induces severe developmental defects (Gabut *et al.* 2007). Downregulation of SR proteins is also detrimental to development. Complete knockout of SR proteins is lethal in mammals (Jumaa *et al.* 1999; Wang *et al.* 2001; Xu *et al.* 2005) and *Drosophila* (Ring and Lis 1994), whereas tissue-specific inactivation of individual SR proteins has revealed specific functions not shared by all members of the SR protein family (Xu *et al.* 2005; Xu and Fu 2005; Sen *et al.* 2013).

Here, we analyzed in detail the consequences of overexpression of SR protein B52 during the development of the mechanosensory bristle cell lineage, at the cellular level. We show that B52 expression level modulates the size, but not the identity, of the cells that make up the bristles. In particular, B52 overexpression increases cell growth and induces strong upregulation of the gene encoding the transcription factor Myc at the transcriptional level. Using a genetic screen, we identified several factors that rescue the phenotypes induced by B52 overexpression, including the tumor suppressor Brain tumor (Brat), which acts as an antagonist of B52 to repress *myc* expression. Our results reveal a role of the SR protein B52 in cell growth and identify several proteins that suppress the deleterious effects of SR protein overexpression on development.

Materials and Methods

Immunostaining and quantification of nuclear area

Dissected nota from 17- to 36-hr-APF pupae were processed as described in Gho *et al.* (1996). The following primary antibodies were used: mouse anti-Cut (DSHB, 1:500); rabbit anti-GFP (Santa-Cruz, 1:500); mouse anti-GFP (Roche, 1:500); rat anti-ELAV (DSHB, 1:100); rat anti-Su(H) (gift from F. Schweisguth, 1:500); mouse anti-Futsch (22C10) (DSHB, 1:100); rabbit anti-Myc d1-717 (Santa Cruz, 1:500); rabbit anti-Lamin (gift from P. Fisher, 1:4000), rat anti-Phospho-tyrosine (Abcam, 1:500), rabbit anti-B52 (Fic *et al.* 2007, 1:1000). Alexa 488- and 568-conjugated secondary antibodies (anti-mouse, -rat, or -rabbit) were purchased from Molecular Probes and used at 1:1000. Cy5-conjugated antibodies (anti-mouse, -rat or -rabbit) were purchased from Promega and were used at 1:2000. Image acquisition was performed using a spinning disc coupled to an Olympus BX-41 microscope (60×, NA 1.25 objective and 40×, NA 0,75 objective) associated with a CoolSnapHQ2 camera (Ropert Scientific), driven by Metamorph software (Universal Imaging). Images were processed with ImageJ software. Quantifications of nuclear area were performed on sensory cells labeled with anti-Cut antibodies that reveal a nuclear protein, or with anti-Lamin antibodies, to delimit nuclei. Image stacks were processed with ImageJ to determine the largest diameter of each nuclei in 3D. Nuclei (50–100) were counted for each cell type and genotype.

Quantification of Myc staining in shaft cells in $B52^{-/-}$ clones (Figure 3B) was done by calculating the correlated total cell fluorescence (CTCF) with ImageJ: CTCF = integrated density – (area of selected cell × mean fluorescence of background). We quantified CTCF at 3 time points (24, 28, and 32 hr APF), using three images per time point. This totals 49 shaft cells, 26 in the clones ($B52^{-/-}$), and 23 outside (control, $B52^{+/-}$). For Figure 5F, CTCF was calculated for 24 cells (12 shafts and 12 sockets). Statistical significance is calculated by *t*-test. Error bars represent SEM.

Chromatin immunoprecipitation (ChIP) analysis on salivary glands

Wild-type or B52-overexpressing salivary glands from third-instar larvae (10 per ChIP assay) were dissected in cold phosphate-buffered saline (PBS) and fixed for 10 min at room temperature in buffer A (50 mM Hepes, 1 mM EDTA, 0.5 mM EGTA, 15 mM NaCl, 60 mM KCl, 0.1% Triton X-100, and Calbiochem protease inhibitor cocktail set I (Merck) containing 1.8% formaldehyde. Crosslinking was stopped by addition of glycine to a final concentration of 0.225 M. Salivary glands were washed three times in cold buffer A and homogenized with a pestle in 300 μl cold buffer B (50 mM Tris-Hcl, pH 7.5, 140 mM NaCl, 1 mM EDTA, 1% NP40, 0.1% SDS, 0.1% sodium deoxycholate, and protease inhibitors) and incubated for 1 hr at 4° on a rotating wheel. Chromatin was sheared by sonication on ice (three times for 30 sec each) with a Vibra-Cell ultrasonic processor (Sonics & Materials) at amplitude 50, followed by 8 min in a Bioruptor sonication system (Diagenode) (pulsed eight times on high for 30 sec, with a 30-sec pause between each pulse). Debris were pelleted by centrifugation for 8 min at maximum speed and 4°. Immunoprecipitations were performed with 150 μl chromatin diluted 1:3 in IP dilution buffer (50 mM Tris-HCl, pH 7.5, 140 mM NaCl, 1 mM EDTA, 1% NP40, and protease inhibitors. We used 20 μl Dynabeads protein G-magnetic beads (Life Technologies) alone or coupled to anti-mouse IgM (Life Technologies). The amounts of antibodies against RNA polymerase II used per immunoprecipitation were 3 μl H14 (Ser5-P), and 5 μl H5 (Ser2-P) (Covance). Beads were washed at room temperature in buffer B containing 140 mM NaCl (3 × 5 min each), 300 mM NaCl (3 × 5 min each), 250 mM LiCl (2 × 5 min each), and then in Tris-EDTA (2 × 5 min each). DNA was eluted at 65° with 300 μl elution buffer (0.1 M $NaHCO_3$ and 1% SDS), with shaking. NaCl was added to 300 mM, and the tubes were incubated for 7 hr at 65° to reverse the crosslinking. After treatment with RNase A (30 min at 37°) and proteinase K (2 hr at 45°), DNA was purified with the Nucleospin extract II kit (Macherey-Nagel) according to the manufacturer's instructions.

ChIP experiments were performed twice using independent chromatin preparations, and quantitative PCR analyses of immunoprecipitated DNAs were performed in triplicate using SYBR Green and a Light Cycler 480 real-time PCR system (Roche). PCR was carried out under conditions of 95° for 2 min, followed by 45 cycles of 95° for 10 sec, 68° for 15 sec, and 72° for 25 sec. Primers used are indicated in Supporting Information, Table S1. The amount of DNA in ChIP samples was extrapolated from a four-point serial

dilution standard curve analysis of chromatin DNA before immunoprecipitation (input). Quantitative PCR values are presented as a percentage of input chromatin, after subtraction of no-antibody control value (IP mock) from the total sample value to eliminate background.

RNA extraction and quantitative RT–PCR

Total RNA was extracted from third-instar larvae or dissected salivary glands using TRI Reagent (Sigma), treated with RQ1-DNase (Promega, Madison, WI), and quantified using a Nanodrop (Wilmington) spectrophotometer. cDNAs were synthesized using the First Strand cDNA kit (GE Healthcare) using 1 μg total RNA as template and $pd(N)_6$ random hexamer primers. Quantitative real-time PCR was performed in a 10-μl reaction mixture in a Light Cycler 480 real-time PCR apparatus (Roche) with SYBR Green and Platinum Taq DNA polymerase (Life Technologies). PCR reactions were carried out under conditions of 95° for 2 min, followed by 45 cycles of 95° for 10 sec, 68° for 15 sec, and 72° for 25 sec. At least two independent samples were collected for each experiment, and each sample was analyzed in triplicate. Relative mRNA levels were calculated by normalization to the levels of ribosomal *rp49* and *Gapdh* mRNAs. Primer sequences are presented in Table S1.

Loss-of-function and overexpression clones

B52 loss-of-function clones were induced using the FLP-FRT technique (Golic and Lindquist 1989) and the following stocks: *y w hs-FLP*; *FRT82B* $B52^{s2249}$*/ TM6B* and *y w ubx-FLP*; *FRT-82B ubi-nls*::*GFP* (gift of J. Knoblich). FLP expression was induced during larval stages and mitotic clones were analyzed at pupal stage. To produce adult clones labeled with *yellow* the following stocks were used: *y w hs-FLP*; *FRT82B* $B52^{s2249}$*/ TM6B* and *y w*; *FRT82B P{Mae-UAS.6.11}*. The *P{Mae-UAS.6.11}* transposon carries a *yellow* reporter gene, therefore, $B52^{s2249}/B52^{s2249}$ clones do not express *yellow*. Two different insertions of this transposon, recovered as negative in our genetic screen, were used to rule out a possible effect of the transposon insertion. Both gave the same results. *B52* gain-of-function clones were induced using the FLIP-out technique (Pignoni and Zipursky 1997) and the following stocks, *y w Act > CD2 > GAL4*; *UAS-GFP*^{mcd8} and *y w hs-FLP*; *UAS-B52*. Images of these clones were acquired on a Zeiss Axioimager Z1 with ApoTome.

Genetic screen

Flies constitutively overexpressing B52 were obtained by combining *GMR–GAL4* or *SOP–GAL4* drivers with the *UAS–B52* transgene, on the same chromosome, to obtain *GMR–GAL4*, *UAS–B52/CyO* and *SOP–GAL4*, *UAS–B52/CyO*, respectively. *GMR–GAL4*, *UAS–B52/CyO* flies were crossed with ~800 *UY* lines containing a random insertion of the *P{Mae-UAS.6.11}* transgene, at 25°. The viability of *GMR–GAL4*, *UAS–B52/UY* flies was calculated by comparison to the sibling *CyO/ UY* flies obtained in the same cross, which generated an average of 100 progeny. *UY* lines significantly and reproducibly rescuing the viability and eye phenotype of *GMR > B52* flies were crossed with *SOP–GAL4*, *UAS–B52/CyO* flies, at 25°. The position of the *UY* element was determined by sequencing the flanking DNA obtained by inverse PCR, according to the Berkeley Drosophila Genome Project (BDGP) protocol.

In two cases (*UY103* and *UY1346*), the insertion maps within a gene in the reverse orientation, which may cause a partial loss of gene function. *UY103* is inserted in the *foraging* (*for*) gene, which encodes a cGMP-dependent protein kinase involved in feeding behavior and neural plasticity. However, targeted expression of an RNAi against *for* [Vienna Drosophila RNAi Center (VDRC) line 108293] did not rescue B52-induced phenotypes in eyes or bristles. Because another gene, *CG34340*, is located 30 kb downstream of the *UAS* sequences and encodes a putative transcription factor of unknown function, it is not clear whether the rescue is due to the insertion within *for* or to misregulation of *CG34340*. This line was not investigated further. In the *UY1346* line, the insertion falls in the *lilliputian* (*lilli*) gene in the reverse orientation, but could also allow forced expression of the upstream gene, *NTPase*, which encodes a nucleoside phosphatase. *UY1346* insertion is homozygous lethal, like *lilli* loss-of-function mutants, suggesting that the insertion may create a partial loss-of-function of *lilli*. Indeed, we observed that expression of an RNAi against *lilli* (VDRC line 106142) strongly suppressed the phenotypes induced by B52 overexpression both in eyes and in bristles (Figure S6). Therefore the rescue obtained with the *UY1346* line is likely due to downregulation of *lilli*.

In the lines *UY2573*, *UY3065*, and *UY3132*, the insertion is very close (<800 bp) to the transcription start site of a candidate gene, in an orientation compatible with forced expression of this gene. Of these, *UY3132* is inserted upstream of the *XNP* gene, which encodes a chromatin remodeler of the SWI2/SNF2 family and significantly rescues the phenotypes induced by B52 overexpression in both tissues. A similar rescue is obtained with the *EP635* line, where the insertion is 20 bp downstream of the *XNP* transcription start site (Figure S6). Therefore, forced expression of XNP is a suppressor of B52-induced phenotypes in both tissues tested.

The insertion in the *UY5158* line lies within a miRNA cluster ~3 kb upstream of the transcription start site of *bancal* (*bl*), which encodes hnRNP K. Because hnRNPs are known antagonists of SR proteins, we anticipated that the rescue was due to misexpression of *bl*. Thus, we tested whether another insertion of a *UAS*-containing transposon in *bl* would rescue B52-induced phenotypes. The insertion *P{EP}*bl^{G13574}, located 55 bp downstream of the *bl* transcription start site, and upstream of the *bl* ATG, gave a rescue similar to *UY5158*; this insertion partially rescues the phenotype induced by B52 overexpression in the eye, but not in bristles (Figure S6). These results strongly suggest that forced expression of hnRNP K, through *UY5158* or *P{EP}*bl^{G13574}, antagonizes B52 overexpression in a tissue-specific manner.

In the last six lines (*UY102*, *UY1131*, *UY4508*, *UY4584*, *UY4739*, and *UY5012*), the insertion maps downstream of

the first transcription start site of a gene, but upstream of its translation start site and in an orientation compatible with forced expression of this gene. Two lines map into the first intron of *Sin3A*, a transcriptional corepressor, and both moderately improve the phenotype induced by B52 overexpression in the eye, but not in the bristles. *UY4584* and *UY4739* map in *Coop* and *jigr1*, respectively, which encode proteins containing a DNA-binding MADF domain (myb/SANT-like domain in Adf-1). *UY102* potentially misregulates *split ends* (*spen*), which encodes a large RNA-binding protein that is found in purified spliceosomes (Herold *et al.* 2009), suggesting possible participation of Spen in RNA splicing. Finally, *UY1131* is inserted in the second exon of the *brain tumor* (*brat*) gene, ~0.3 kb upstream of an alternative *brat* promoter. We confirmed that Brat overexpression is responsible for the rescue of the phenotypes using a *UAS–Brat* transgene (Sonoda and Wharton 2001) as shown in Figure 5.

Results

Cell growth is increased after B52 overexpression in the bristle cell lineage

To precisely determine the function of B52 at the cellular level, we first analyzed the consequences of B52 overexpression during development of the external mechanosensory organs. Mechanosensory bristles, located on the dorsal surface of the fly, comprise two populations, microchaetes and macrochaetes, which are short and long bristles, respectively. Each organ is composed of two outer cells, the socket and shaft cells, and two inner cells, the neuron and sheath cell. All four cells arise from a precursor cell after four asymmetric divisions during early pupal development, and they differ in size, location in the cluster, and expression of specific markers (Figure 1A). Immunostaining revealed that B52 is expressed throughout the bristle cell lineage. B52 protein is detected at similar levels in the nuclei of all precursor and differentiated cells and accumulates preferentially in the shaft cell at the final stages of development in macrochaetes (Figure 1B).

We overexpressed B52 in the bristle lineage under the control of the *SOP–GAL4* and *neuralized*^{P72}*–GAL4* (*neur*^{P72}*–GAL4*) drivers (Figures 1 and Figure S1). B52 overexpression under the control of these promoters gives rise to viable flies and to pharat adults respectively. *SOP > B52* adults display a partial loss of thoracic macrochaetes, in which only the sockets are present compared to wild type (Figure 1C). This phenotype is quantifiable by counting the remaining dorsocentral and scutellar macrochaetes on the thorax. Wild-type flies have four of each type of macrochaete, *i.e.*, eight bristles. In *SOP > B52* flies, ~70% of males and females have two to five macrochaetes, and only 2% of males and no females have eight bristles (Figure 1C). In the *neur*^{P72} *> B52* context, no sockets or shafts are observed, and pharat adults are devoid of almost all microchaetes and macrochaetes (Figure S1A). These results indicate that the *neur*^{P72}*–GAL4* driver is stronger than the *SOP–GAL4* driver and that B52 expression level must be precisely controlled to ensure the normal development of the bristles.

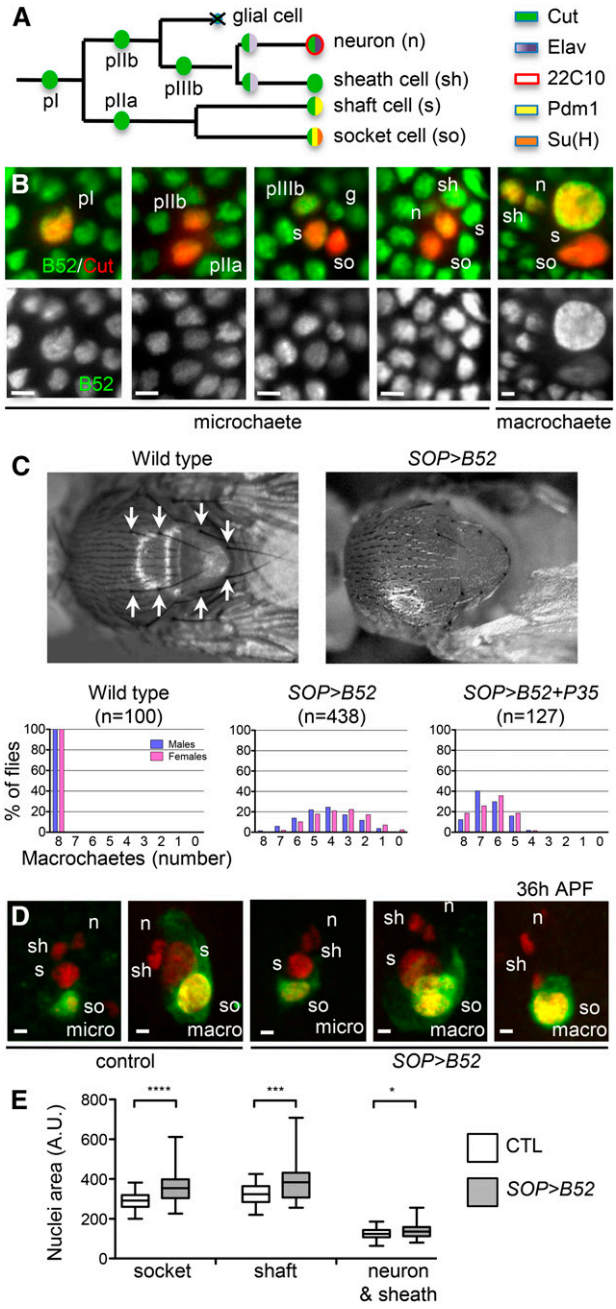

Figure 1 B52 overexpression induces cell growth. (A) Schematic representation of the wild-type bristle lineage and cell markers used. (B) B52 protein expression in microchaete and macrochaete bristle lineage cells at progressive stages of development (16 to 24 hr after pupae formation, APF). (C) Eight macrochaetes present on a wild-type fly thorax are indicated by arrows. *SOP > B52* flies show a variable loss of macrochaetes, as exemplified by the image showing a fly with only one of the eight macrochaetes remaining. Histograms show the distribution of the flies according to the number of macrochaetes. The numbers of flies of each genotype are indicated in parentheses. (D) Immunostaining of sensory clusters of microchaetes (micro) and macrochaetes (macro) from control and *SOP > B52* pupae. Images were captured 24 hr APF, with the exception of the 36-hr image on the right. Note that the cluster from 36-hr-APF pupae contains only three cells; the shaft cell is missing; and the size of the nuclei is slightly increased after B52 overexpression. Scale bars, 2 μm. (E) Quantification of the nuclear area of the bristle lineage cells in control (CTL, *SOP–GAL4/+*) and *SOP > B52* (*SOP–GAL4*, *UAS–B52 /+*) pupae. Neuron and sheath cells were not discriminated and were included in the same pool.

Absence of external structures can result from a defect in cell proliferation, cell identity, or cell death during development of the bristle cell lineage. Therefore, we analyzed this lineage at the cellular level, using several markers, in pupae overexpressing B52. We always detected the normal number of cells and appropriate expression of markers, indicating that B52 overexpression does not modify the identity of the cells in the lineage of microchaetes and macrochaetes at 24 hr after pupae formation (APF) (Figures 1D and Figure S1). Later, at 30–36 hr APF, clusters devoid of shaft cells are observed in macrochaetes in *SOP > B52* pupae and in both microchaetes and macrochaetes in $neur^{P72}$ *> B52* pupae (Figure 1D and Figure S1). This correlates with the adult phenotype showing partial loss of bristles. The absence of macrochaete bristles in *SOP > B52* adults is partially rescued by co-overexpression of the caspase inhibitor P35, indicating that the shaft cell dies through apoptosis (Figure 1C). It should be noted that B52 expression is the highest in the macrochaete shaft cell (Figure 1B), which may explain why this cell is the most sensitive to B52 overexpression. We observed that, whereas the identity of the cells in this lineage is not affected by B52 overexpression, the cells appeared slightly larger than wild-type cells. To quantify this phenotype, we measured nuclear area in the cells, because nuclear volume is proportional to cell volume (Walters *et al.* 2012) and observed that *SOP > B52*-overexpressing cells have larger nuclei than control cells (Figure 1E). The mean nuclear area is increased upon B52 overexpression by 12% in neuron and sheath cells, by 19% in shaft cells, and by 24% in socket cells. These observations were confirmed with the $neur^{P72}$*–GAL4* driver (Figure 5C). Taken together, these results show that B52 overexpression increases cell growth and eventually induces cell death in the bristle lineage.

Cell growth and Myc expression are reduced after B52 depletion

We next analyzed the consequences of B52 knockdown on development of the bristle lineage. We generated homozygous *B52* mutant cell clones in heterozygous $B52^{s2249}/+$ flies by somatic recombination. As expected, B52 protein is not detected in $B52^{s2249}/B52^{s2249}$ mutant clones visualized by the lack of GFP (Figure 2A). Within mutant clones, the bristle cell lineage develops normally, as indicated by the detection, at different time points during pupal development, of the precursor cells and the four differentiated cells expressing the appropriate markers (Figure 2, A–C). Nevertheless, we observed a slight delay in the bristle cell lineage progression and in the differentiation of the clusters in *B52* mutant clones. For example, Figure 2A shows clusters containing only two cells in *B52* mutant clones, whereas clusters outside of the clone have three or four cells. Desynchrony between *B52* mutant and wild-type clusters is also revealed by staining with the neuronal marker Elav. Figure 2B shows that Elav staining is weak and not yet restricted to the neuron in *B52* mutant clones, whereas the neuron is more strongly stained in wild-type clusters. Therefore, B52 depletion does not impair differentiation of this lineage, but delays its development. Interestingly, we observed that *B52* mutant cells appear smaller than heterozygous cells, as demonstrated by staining of the apical periphery with anti-phosphotyrosine antibody (Figure 2D). Quantification of the nuclear area of epithelial cells reveals that growth retardation increases with pupal age (Figure 2E). This is likely due to the dilution of B52 protein present in the founder cell as the clone divides and to the growth of epithelial cells, which occurs late (after 24 hr APF) in development. In agreement with this decrease in cell growth, adult *B52* mutant organs have smaller bristles, as shown in Figure 2F. These data indicate that cell growth is impaired in the *B52* loss-of-function background.

This phenotype of reduced bristle size is reminiscent of *myc* hypomorphic mutants, which also display smaller and thinner bristles (Johnston *et al.* 1999). The transcription factor Myc is a major regulator of growth in *Drosophila* and controls ribosome biogenesis (Oskarsson and Trumpp 2005). We, therefore, analyzed whether B52 depletion modulates Myc expression level in the bristle lineage. In the wild type, Myc is mainly detected in the sublineage generating the outer cells (Figure 3A). At 16 hr APF, Myc is first detected in the pI precursor cell at a level comparable to that in the surrounding epithelial cells and then accumulates in the pIIa precursor cell at 18 hr APF. Just after pIIa division, Myc is found in both daughter cells (the socket and the shaft) and later accumulates in the shaft cell at 22–24 hr APF. In *B52* mutant clones, we did not detect a significant difference in Myc staining in epithelial cells, but observed a slight decrease in staining in cells of several lineage clusters, suggesting that B52 depletion decreases Myc expression in these cells (Figure 3B). Comparison of Myc staining between shaft cells, within and outside the clones, reveals a 35% decrease of Myc level in $B52^{-/-}$ cells. Because B52 depletion delays formation of the clusters, as indicated by weak staining with the neuron-specific marker 22C10 (Figure 3B), the decreased level of Myc could be a consequence of this delay. To further address whether B52 depletion decreases Myc expression, we analyzed *myc* mRNA level in *B52* mutant larvae, which die at the third-instar larval stage. We observed that mutant larvae express decreased levels of *myc* mRNA and pre-mRNA (Figure 3C). This suggests that the slight decrease in Myc protein level observed in the shaft cell in *B52* mutant clones is not due only to a developmental delay. Given that we do not see a decrease of Myc staining in $B52^{-/-}$ epithelial cells but only in the shaft cell, our results suggest that B52 depletion decreases *myc* expression in a tissue-specific manner.

B52 overexpression upregulates Myc at the transcriptional level

We next asked whether B52 overexpression also affected Myc expression, because B52 overexpression in the bristle lineage increases cell size. We observed that B52 overexpression strongly increased Myc staining in the four cells of the lineage (Figure 3D). To determine at which level (transcriptional or post-transcriptional) B52 can affect *myc* expression, we looked for another tissue that is more suitable for molecular analyses. We had previously observed that B52 overexpression in salivary glands increases, and B52 depletion reduces, nuclear size (Juge

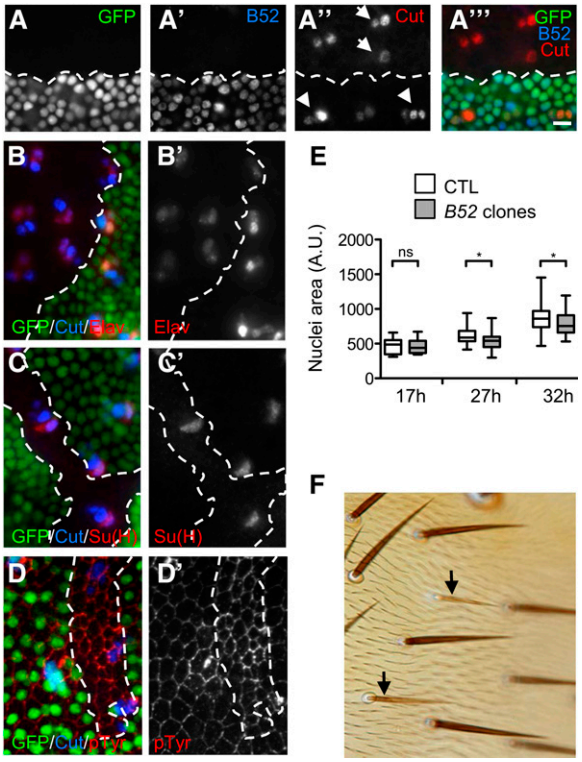

Figure 2 B52 depletion delays cluster development and reduces cell growth. (A–D) *B52*^{s2249} somatic clones are detected by the lack of green fluorescent protein (GFP). Boundaries between clones and control cells are shown with white dashed lines. (A) Immunostaining of 21-hr-old pupae showing that B52 protein is not detected in *B52*^{s2249} somatic clones. Note that clusters in *B52*^{s2249} clones contain only one or two cells (arrows), whereas control clusters contain three or four cells (arrowheads). (B) Expression of the neuronal marker Elav (23-hr-old pupae). (C) Expression of the socket marker Su(H) (24-hr-old pupae). (D) Immunostaining of 24-hr-old pupae with anti-phospho-tyrosine antibody (pTyr), which labels cells apical periphery, shows that cells are smaller in *B52*^{s2249} somatic clones. (A–D) Scale bars, 10 μm. (E) Quantification of nuclei area of epithelial cells in nota from 17-hr, 27-hr, and 32-hr-old pupae in *B52*^{s2249} homozygous mutant clones compared to surrounding heterozygous cells (CTL). (F) External sensory organs (microchaetes) in mosaic flies. *B52*^{s2249} homozygous mutant organs are identified by their yellow phenotype (arrows).

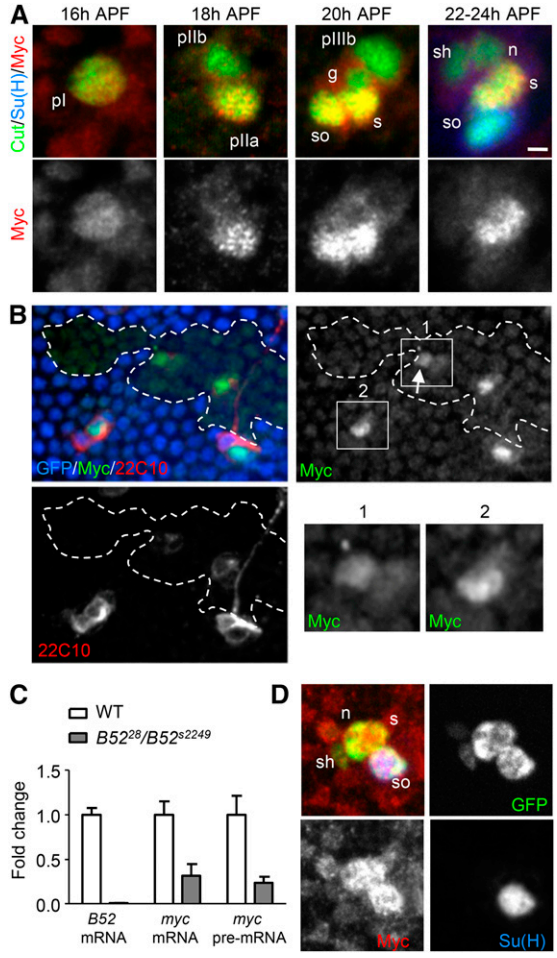

Figure 3 B52 expression level modulates *myc* expression. (A) Expression pattern of Myc protein in wild-type bristle cell lineage between 16 and 24 hr APF. (B) Myc expression in *B52*^{s2249} somatic clones. *B52*^{s2249} clones are detected by the lack of GFP (false colored in blue). Boxes labeled 1 and 2 represent a zoom in on two lineage clusters, in the clone (1, *B52*$^{-/-}$) and outside (2, *B52*$^{+/-}$). (C) Quantification of *myc* mRNA and pre-mRNA levels by qRT–PCR in wild-type and *B52* mutant larvae (*trans*-heterozygous *B52*^{s2249} over a deficiency *B52*^{28} of *B52* locus). (D) Myc expression in bristle lineage cells overexpressing B52 (*neur*^{P72}>*B52*) at 24 hr APF.

et al. 2010), suggesting that B52 expression level may also influence cell growth in this organ. To determine whether B52 overexpression leads to Myc upregulation in salivary gland, we induced B52 overexpression in individual cells with the *Act* > *CD2* > *GAL4* driver, which is turned on by excision of a stop cassette (CD2) upon expression of a heat-inducible flippase. Cells overexpressing B52 are larger and display stronger Myc staining than control cells (Figure 4A). This finding shows that, as in the bristle lineage, overexpression of B52 induces Myc overexpression in salivary gland cells in a cell-autonomous manner.

To determine whether B52 modulates *myc* expression at the transcriptional or post-transcriptional level, we analyzed levels of *myc* mRNA and pre-mRNA by qRT–PCR. To this end, we overexpressed B52 in all cells of the salivary gland using the *sgs3–GAL4* driver, which drives the expression of GAL4 in this organ from the mid-third-instar larval stage. Salivary glands overexpressing B52 display larger nuclei than control cells (Figure 4B), and *myc* mRNA and pre-mRNA are strongly upregulated (Figure 4C). This observation suggests an effect of B52 on *myc* transcription. This conclusion is supported by the observation that B52 overexpression increases expression of a *LacZ* enhancer trap (*dm*^{G0139}) inserted in the *myc* locus, both in salivary glands (Figure 4D) and in the bristle lineage (Figure S2). To further confirm that *myc* transcription is upregulated by B52, we used chromatin immunoprecipitation (ChIP) to analyze the distribution of RNA polymerase II (Pol II) on the *myc* locus in wild-type and B52-overexpressing salivary glands. We used antibodies recognizing the phosphorylated Ser5-P and Ser2-P forms of the Pol II carboxyterminal domain (CTD), which are associated with the initiation and elongation phases of transcription, respectively. In wild-type salivary glands, Pol II Ser5-P is detected primarily around the transcription start site of the *myc* locus (Figure 4E). This site likely corresponds to a Pol II

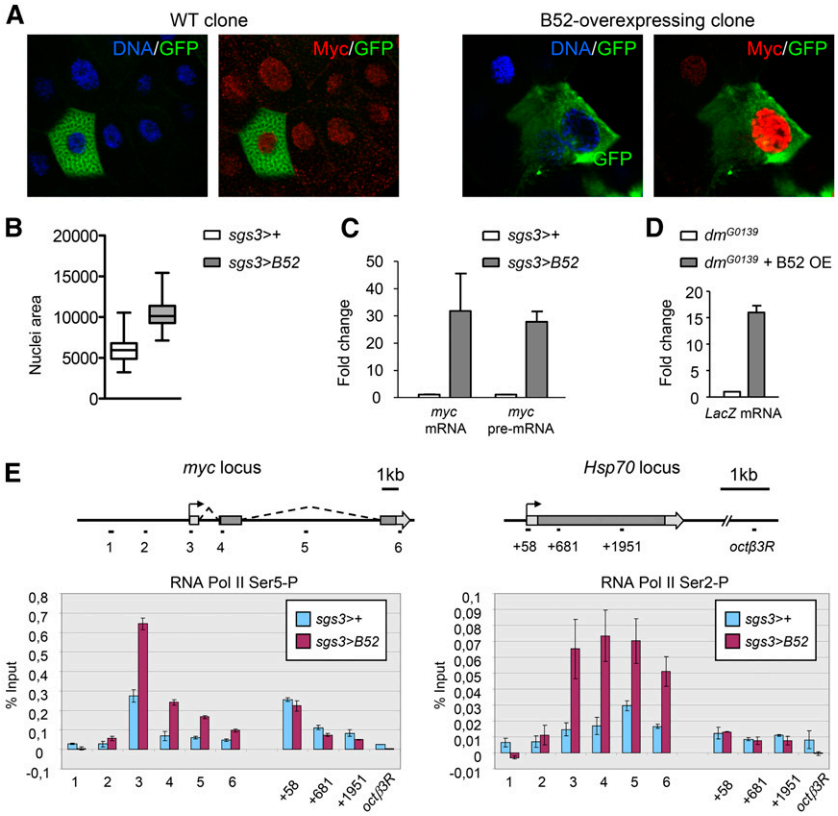

Figure 4 B52 overexpression increases *myc* transcription in salivary glands. (A) Immunodetection of Myc (red) in a control wild-type (WT) cell clone (left, genotype: *hs-FLP/act[CD2]GAL4*; *UAS–GFP/+*) and a B52-overexpressing cell clone (right, genotype: *hs-FLP/act[CD2]GAL4*; *UAS–GFP/UAS-B52*). The single cell in which Act–GAL4 is turned on is labeled by the presence of GFP (green). Nuclei are stained with DAPI (blue). (B) Quantification of nuclear area in control salivary glands (open box, *sgs3–GAL4/+*) and B52-overexpressing salivary glands (shaded box, *sgs3–GAL4/UAS–B52*). (C) Quantification of *myc* mRNA and pre-mRNA levels by qRT–PCR in control (white box, *sgs3–GAL4/+*) and B52-overexpressing salivary glands (gray box, *sgs3–GAL4/UAS–B52*). (D) Quantification of *LacZ* mRNA level by qRT–PCR in dm^{G0139} male salivary glands in the absence (white box, genotype: dm^{G0139}; *sgs3–GAL4/+*) or presence (gray box, genotype: dm^{G0139}; *sgs3–GAL4/UAS–B52)* of B52 overexpression. (E) Distribution of RNA Pol II over *myc* and *hsp70* loci determined by ChIP analysis in control (blue, *sgs3–GAL4/+*) or B52-overexpressing salivary glands (purple, *sgs3–GAL4/UAS–B52*). The positions of the amplified fragments are indicated below the drawing of each locus.

pause site that has been observed in embryos (Muse *et al.* 2007). Indeed, we observed a similar enrichment of Pol II Ser5-P at the well-characterized pause site in the *hsp70* locus (Figure 4E). Overexpression of B52 increased Pol II Ser5-P in the proximal promoter region of the *myc* locus and strongly increased the Pol II Ser2-P signal in the coding region, consistent with enhanced *myc* transcription. B52 overexpression did not modify the Pol II profile on *hsp70* (Figure 4E), ruling out the possibility that B52 globally affects Pol II pausing. Together, these findings show that B52 overexpression, directly or indirectly, increases *myc* expression at the transcriptional level.

Genetic screen identifies suppressors of the phenotypes induced by B52 overexpression

To gain insight into the links between B52 and cell growth, we sought to identify suppressors of the B52 overexpression-induced phenotypes. Indeed, we previously showed that overexpression of DNA topoisomerase I, which acts as a kinase for SR proteins, rescues these phenotypes in the eye (Juge *et al.* 2010). Therefore, a gain-of-function screen appeared suitable to identify suppressors of the defects induced by B52 overexpression. We designed a genetic screen to look for proteins that rescued the phenotypes induced by B52 targeted overexpression in two different organs, the eye and bristles. We developed transgenic lines constitutively overexpressing B52 in the eyes (*GMR–GAL4* driver) or sensory bristles (*SOP–GAL4* driver). *GMR > B52* flies have reduced viability (Table 1) and display eyes that are greatly reduced in size, disorganized, and depigmented (Figure S3), whereas *SOP > B52* flies are fully viable and display a partial loss of thoracic macrochaetes, which is quantified as described in Figure 1C. As a control, we expressed an inhibitory aptamer RNA [iaRNA, encoded by the transgene *UAS–BBS(5.12)*] that contains stretches of high-affinity binding sites for B52 and has been shown to titrate B52 *in vivo* (Shi *et al.* 1999). As expected, targeted coexpression of this transgene almost completely rescued the phenotypes induced by B52 overexpression driven by *GMR–GAL4* or *SOP–GAL4* (Figure S3). This result indicates that both phenotypes involve the RNA-binding activity of B52.

We screened a collection of transgenic flies carrying a random insertion of the *P{Mae-UAS.6.11}* element, which contains *UAS* sequences and a minimal promoter at one end of the transposon. In the presence of GAL4, this transgene allows forced expression of the gene located downstream of its insertion point in the genome. We randomly screened ~800 lines and recovered 12 lines that significantly improved the size of the eyes of B52-overexpressing flies and rescued their viability (Table 1 and Figure S4). These lines were then tested for rescue of the phenotype induced by B52 overexpression in the bristle cell lineage (Figure S5). The outcome of the two screens is summarized in Table 1. Of the 12 lines identified, 8 significantly rescued the phenotypes induced by B52 overexpression in both eye and bristles, whereas the other four showed tissue-specific rescue in the eye only. We mapped the transgene insertion point in each of the 12 positive lines by inverse PCR. In most cases (10/12), the orientation of the insertion is compatible with overexpression of the target gene (insertion upstream of a promoter and of an ATG of the target

Table 1 Characteristics of the positive *UY* lines identified in the genetic screen

	GMR-Gal4		*SOP-Gal4: rescue*[a]					
	Viability (%)							
UY line	M	F	Rescue[a]	Gene name	CG number	Insertion[b]	Direction[c]	Function
none	48	18	–	–				
UY102	52	61	++	++	*split ends (spen)*	CG18497	+1.8 kb	+	RNA binding
UY103	67	50	+++	+	*foraging (for)*	CG10033	+24.8 kb	–	Protein kinase
UY1131	74	43	+++	+	*brain tumor (brat)*	CG10719	+24.7 kb	+	Translational repressor
UY1346	78	61	+++	++	*lilliputian (lilli)*	CG8817	+2.8 kb	–	Transcription factor
UY2573	91	71	+	+++	*jumeau (jumu)*	CG4029	−4 nt	+	Transcription factor
UY3065	70	80	++	–	*kuzbanian (kuz)*	CG7147	−0.8 kb	+	Metalloprotease
UY3132	87	85	++	++++	*xnp*	CG4548	−0.2 kb	+	Chromatin remodeler
UY4508	55	35	+	–	*Sin3A*	CG8815	+3 kb	+	Transcriptional corepressor
UY4584	75	100	++	++++	*corepressor of Pan (coop)*	CG1621	+0.2 kb	+	Transcriptional corepressor
UY4739	91	100	++	+++	*jing interacting gene regulatory 1 (jigr1)*	CG17383	+9.5 kb	+	DNA binding
UY5012	60	50	+	–	*Sin3A*	CG8815	+4.5 kb	+	Transcriptional corepressor
UY5158	69	64	+++	–	*bancal (bl)*	CG13425	−3 kb	+	RNA binding

[a] The phenotypic rescue is empirically ranked from – (no rescue) to ++++ (near wild type) according to our appreciation of the phenotypes.
[b] Position of the transposon insertion point relative to the first transcription start site of the candidate gene (+, downstream; –, upstream)
[c] Orientation of the *UAS* sequences relative to the transcription of the target gene: +, compatible with overexpression; –, reverse orientation.

gene); however, in two cases (*UY103* and *UY1346*), the insertion maps within a gene in the reverse orientation. The identities of the genes likely responsible for the rescue of the phenotypes induced by B52 overexpression are indicated in Table 1. Using other gain- or loss-of-function lines, we confirmed the identity of Brat, Lilli, Xnp, and Bancal as suppressors of B52 overexpression-induced phenotypes (see *Materials and Methods* and Figure S6).

Interestingly, among the candidates proteins identified, Lilli and Brat were previously shown to affect cell growth. Lilli has a positive effect on growth (Wittwer *et al.* 2001), and Brat is a negative regulator of growth (Frank *et al.* 2002). In the *UY1346* line, the insertion falls in the *lilli* gene in the reverse orientation. This insertion is homozygous lethal, like *lilli* loss-of-function mutants, suggesting that the insertion may create a partial loss-of-function of *lilli*. We tested whether *lilli* depletion by RNAi would rescue the phenotypes induced by B52 overexpression. Indeed, we observed that expression of RNAi targeting *lilli* strongly suppressed the phenotypes induced by B52 overexpression in both eye and bristles (Figure S6). In the *UY1131* line, the transposon is inserted in the second exon of the *brat* gene, ~0.3 kb upstream of an alternative *brat* promoter. *brat* is a tumor-suppressor gene that negatively regulates cell growth (Frank *et al.* 2002) and acts as a post-transcriptional repressor of *myc* (Betschinger *et al.* 2006; Harris *et al.* 2011). The identification of Brat as a potent suppressor of the phenotypes induced by B52 overexpression is particularly interesting because our results show that B52 overexpression increases cell growth and *myc* expression in several tissues. We, therefore, investigated this candidate further.

B52 and Brat act antagonistically on myc expression in the bristle lineage

To confirm that forced expression of Brat in the *UY1131* line is responsible for the phenotypic rescue, we used a *UAS–brat* transgene (Sonoda and Wharton 2001) to drive overexpression of a *brat* cDNA. This transgene rescues the phenotypes induced by B52 overexpression both in the eye (Figure 5A) and in the bristles (compare Figure 1C and Figure 5B), at a level similar to that seen in the *UY1131* line. This confirmed that Brat overexpression antagonizes the effect of B52 overexpression in these two organs. We showed (Figure 1E and Figure 3D) that B52 overexpression in the bristle cell lineage induces an increase in cell size and ectopic accumulation of Myc protein. Because Brat is a negative regulator of *myc* expression, we investigated whether Brat overexpression would rescue this phenotype. We observed that Brat overexpression reduced the size of nuclei in cells overexpressing B52 (Figure 5C) and reduced nuclear expression of Myc in these cells (Figure 5, E and F). Overexpression of Brat alone in the lineage induces a very slight decrease of socket cell size but not of the other cells (Figure 5C). Moreover no bristle phenotype is detected in adults (Figure S7) indicating that Brat overexpression alone does not significantly affect bristle lineage development. Together, our results show that Brat overexpression counteracts the effect of B52 on *myc* expression and growth and rescues the shaft cell death induced by B52 overexpression.

Our results raise the possibility that the upregulation of Myc could be responsible for the phenotype induced by B52 overexpression in the bristle lineage. We therefore investigated whether reducing Myc level, either by using a hypomorphic *myc* mutants (dm^1) or by expressing an RNAi against *myc* (2 UAS–RNAi lines used) would rescue the phenotypes due to B52 overexpression in bristles. In all cases we see that these contexts do not rescue the phenotype but instead slightly increase it (data not shown). As B52 overexpression induces cell death (Gabut *et al.* 2007; this study), it seems that downregulating *myc* in this context favors the apoptotic program induced by B52, by an unknown mechanism. Finally, to further address whether Myc upregulation on its own could be

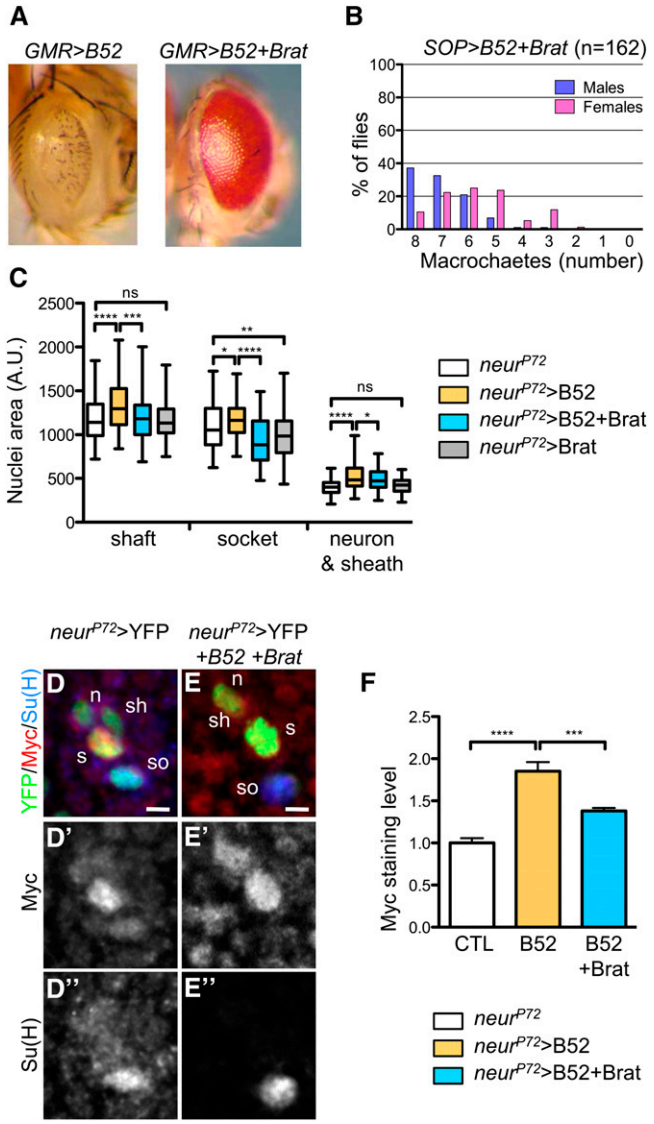

Figure 5 Brat overexpression rescues the phenotypes induced by B52 overexpression. (A) Eye pictures of flies overexpressing B52 (left) and co-overexpressing B52 and Brat (right) under the control of *GMR–GAL4*. (B) Quantification of the bristles phenotype of flies co-overexpressing B52 and Brat. Compare to Figure 1C. (C) Quantification of nuclear area of microchaete lineage cells in control, B52-overexpressing, and B52- and Brat-overexpressing pupae. Expression is driven by the $neur^{P72}$*–GAL4* driver. (D and E) Expression pattern of Myc in the bristle cell lineage 24 hr APF, in control (D, D′, D′′) and in $neur^{P72}$ > *Brat,B52* pupae (E, E′, E′′). Sensory cells were identified by expression of yellow fluorescent protein (YFP), and socket cells were labeled with anti-Su(H). Scale bars, 2 μm. (F) Quantification of Myc immunostaining level in bristle and shaft cells, in control, B52-overexpressing, and B52- and Brat-overexpressing pupae.

responsible for the phenotype induced by B52 in the bristle lineage, we overexpressed a *myc* cDNA under the control of the *SOP–Gal4* driver. Overexpression of Myc alone in this lineage induces a very weak phenotype compared to B52 overexpression, with 37% of males and 19% of females lacking only one macrochaete bristle (Figure S7). This phenotype is almost completely rescued by Brat overexpression, confirming the antagonism between Brat and Myc in this lineage (Figure S7). Altogether these results show that Myc overexpression is not solely responsible for the phenotypes induced by B52 overexpression in this lineage and strongly suggest that Brat, as well as other suppressors identified in the screen, antagonizes B52 effects at multiple levels.

Discussion

Here, we used the *Drosophila* bristle cell lineage as a model to analyze the consequences of modulating B52 protein level on development and differentiation and to identify factors capable of antagonizing the effects of SR protein overexpression *in vivo*. Overexpression of B52 during development in this lineage gives rise to flies lacking few to most of the thoracic bristles. At the cellular level, we observed that this phenotype is not due to an alteration of the differentiation program of this lineage, but rather to the death of the shaft cell. In fact, neither upregulation nor loss-of-function of B52 modified the identity of the cells in this lineage in our experiments. On the other hand, we observed that modulation of B52 expression level modifies cell size; B52 depletion reduced cell size in the bristle lineage (Figure 2, D and E) and in salivary gland (Juge *et al.* 2010), whereas B52 overexpression in these cells/organs increased cell size (Figure 1E and Figure 4B). These findings reveal a role of this SR protein in cell growth modulation. We used a genetic screen to identify proteins that can rescue the phenotypes induced by overexpression of B52 in the bristles and the eyes and identified several candidates. Except for an hnRNP (Bancal), none of these factors are known antagonists of SR proteins functions. Interestingly, two candidate genes, *lilli* and *brat*, have been previously implicated in cell growth. Whereas *brat* is a negative regulator of growth (Frank *et al.* 2002), *lilli* was shown to have a positive effect on cell growth (Wittwer *et al.* 2001). Our results show that loss-of-function of *lilli* and overexpression of *brat* can rescue the phenotypes induced by B52 overexpression, in agreement with the positive effect of B52 on cell growth.

As Myc transcription factor plays a major role in the control of cell growth in *Drosophila*, we analyzed whether *myc* expression was affected by B52 level. We observed that B52 overexpression induced a strong upregulation of Myc in several tissues (Figure 3 and Figure 4), whereas *myc* RNA level is reduced in *B52* mutants (Figure 3). Moreover, we show that overexpression of Brat, a known post-transcriptional repressor of *myc*, restores Myc protein level and cell size in the B52-overexpressing bristle cell lineage and rescues the phenotype in adults. Interestingly, other candidates identified in the screen have a link with Myc in mammals. The Lilli homolog, AFF4, is a central subunit of the super elongation complex (SEC) involved in transcription elongation (Luo *et al.* 2012a). *c-myc* is one of the direct targets of AFF4/SEC, and SEC recruitment to the *c-myc* gene regulates its expression in several cancer cells (Luo *et al.* 2012b). In mammals, Sin3A causes deacetylation of Myc and represses Myc activity (Nascimento *et al.* 2011). Knockdown of *Sin3A* in *Drosophila* S2 cells increases expression of a Myc-dependent reporter (Furrer *et al.*

2010), suggesting that it may also antagonize Myc activity in *Drosophila*. Finally, hnRNP K, the mammalian homolog of Bancal, binds to *c-myc* promoter (Tomonaga and Levens 1995) and acts as a transcription factor (Michelotti *et al.* 1996). These data suggest that B52 effects on growth are mediated, at least in part, by its consequences on *myc* expression level. Unfortunately our attempts to rescue the phenotypes induced by B52 overexpression, by expressing RNAi against *myc*, or in *myc* mutant background, did not succeed. This could be due to an insufficient reduction of *myc* to compensate the upregulation induced by B52. This could also reveal that B52 overexpression affects other pathways involved in cell growth and/or apoptosis. In addition, we observed that Myc upregulation alone in the bristle lineage induces a very weak phenotype compared to B52 (Figure S7). Despite the fact that the level of overexpression of Myc is probably not exactly the same in these two situations, this result also suggests that the phenotypes induced by B52 overexpression are not due to the sole upregulation of Myc. Therefore B52 overexpression is likely to affect expression of additional genes modulating cell growth and cell death. We speculate that the suppressors identified in our screen, including Brat, antagonize B52 effects by acting on multiple targets and/or at multiple levels. Notably, half of these suppressors encode transcription factors, suggesting that particular transcriptional programs may counteract the effects of B52 overexpression in specific tissues.

The high level of *myc* overexpression induced by B52 overexpression, especially in the salivary gland (Figure 4C), raises the question of how B52 expression level modulates *myc* transcription. Since B52 overexpression can alter alternative splicing (Fic *et al.* 2007; Gabut *et al.* 2007), it may modify the expression of mRNAs encoding regulators of *myc* transcription. Identification, by RNAseq, of the alternative splicing events modulated by B52 level *in vivo* should allow to identify the alternative splicing program controlled by this SR protein and shed light on the potential targets involved in cell growth and apoptosis. An alternative, but not mutually exclusive, hypothesis would be that B52 directly participates in *myc* transcription. Recently Ji *et al.* (2013) identified a role of the mammalian SR proteins SRSF1 and SRSF2 in the release of transcription pausing. SRSF1 and SRSF2 interact at promoters with the 7SK snRNP, which sequesters the elongation factor P-TEFb (cdk9/cyclinT complex) in an inactive complex. Release of SR protein from the 7SK snRNP, likely mediated by the transcribed nascent RNA, also releases P-TEFb, which may then associate with other subunits of the SEC to promote transcription elongation (Ji *et al.* 2013). SRSF2 depletion reduces recruitment of both cdk9 and AFF4 to most (4/5) promoters studied, indicating that SEC recruitment is diminished (Ji *et al.* 2013). Interestingly, we show that downregulation of Lilli, the *Drosophila* homolog of AFF4, efficiently rescues the phenotypes induced by B52 overexpression *in vivo* (Figure S6). It is therefore possible that overexpression of B52 participates in the release of Pol II from pause at the *myc* promoter, either through titration of inhibitory factors, such as the 7SK snRNP, or through enhanced recruitment of SEC components. This effect would be promoter specific because we observed that distribution of paused Pol II is not altered on the *hsp70* gene (Figure 4E) and, consistent with this, we previously showed that B52 overexpression does not induce *hsp70* expression (Juge *et al.* 2010). In agreement with antagonism between B52 and the SEC, we observed that depletion of ELL (a partner of Lilli in the SEC) by RNAi also rescues the phenotypes induced by B52 overexpression, similarly to *lilli* RNAi (Figure S6). These results suggest that a link between SR proteins and the SEC also exists in *Drosophila*. Unfortunately, our attempts to analyze the distribution of B52 on the *myc* locus by ChIP were unsuccessful due to poor performance of the B52 antibody in immunoprecipitation. Because all components of the 7SK snRNP and SEC are conserved in *Drosophila*, it will be interesting to determine whether the function of SR proteins in transcription pausing and elongation is conserved in this organism.

Our results highlight a new role of the SR protein B52 in cell growth and identify a link between B52 and Myc expression levels. Interestingly, a similar correlation has been identified in mammals, but in that case, Myc was shown to directly regulate SRSF1 transcription (Das *et al.* 2012). It has been shown that upregulation of SRSF1 and SRSF6 contribute to Myc oncogenic potential (Das *et al.* 2012; Cohen-Eliav *et al.* 2013). Therefore, coordination between the Myc transcription program and specific alternative splicing events regulated by these SR proteins appears to be important in promoting cell transformation. Elucidation of the splicing program regulated by B52 during development of specific tissues will provide crucial insights into further understanding the role of this protein in cell growth.

Acknowledgments

We thank Martine Simonelig, Jean-Maurice Dura, and Magalie Lecourtois for providing us *P{Mae-UAS.6.11}* transgenic lines; Robin Wharton for *UAS–Brat* transgenic lines; the Vienna Drosophila RNAi Center for the RNAi lines; and the Bloomington Drosophila Stock Center for other transgenic lines. We thank the Montpellier RIO Imaging facility for microscopy. This work was supported by grants from the European Alternative Splicing Network of Excellence (EURASNET, FP6 life sciences, genomics and biotechnology for health), the Institut National du Cancer (Cancéropôle Ile-de-France), and the Association pour la Recherche contre le Cancer ARC (award no. 4894 to François Juge). C. Fernando was a recipient of a fellowship from the Ministry of National Education, Research and Technology (M.E.N.R.T) and the Association pour la Recherche contre le Cancer (ARC). The authors declare that they have no conflict of interest.

Literature Cited

Betschinger, J., K. Mechtler, and J. A. Knoblich, 2006 Asymmetric segregation of the tumor suppressor brat regulates self-renewal in Drosophila neural stem cells. Cell 124: 1241–1253.

Chen, M., and J. L. Manley, 2009 Mechanisms of alternative splicing regulation: insights from molecular and genomics approaches. Nat. Rev. Mol. Cell Biol. 10: 741–754.

Cohen-Eliav, M., R. Golan-Gerstl, Z. Siegfried, C. L. Andersen, K. Thorsen *et al.*, 2013 The splicing factor SRSF6 is amplified and is an oncoprotein in lung and colon cancers. J. Pathol. 229: 630–639.

Das, S., O. Anczuków, M. Akerman, and A. R. Krainer, 2012 Oncogenic splicing factor SRSF1 is a critical transcriptional target of MYC. Cell Reports 1: 110–117.

Fic, W., F. Juge, J. Soret, and J. Tazi, 2007 Eye development under the control of SRp55/B52-mediated alternative splicing of eyeless. PLoS ONE 2: e253.

Frank, D. J., B. A. Edgar, and M. B. Roth, 2002 The Drosophila melanogaster gene brain tumor negatively regulates cell growth and ribosomal RNA synthesis. Development 129: 399–407.

Furrer, M., M. Balbi, M. Albarca-Aguilera, M. Gallant, W. Herr *et al.*, 2010 Drosophila Myc interacts with host cell factor (dHCF) to activate transcription and control growth. J. Biol. Chem. 285: 39623–39636.

Gabut, M., J. Dejardin, J. Tazi, and J. Soret, 2007 The SR family proteins B52 and dASF/SF2 modulate development of the Drosophila visual system by regulating specific RNA targets. Mol. Cell. Biol. 27: 3087–3097.

Gho, M., M. Lecourtois, G. Géraud, J. W. Posakony, and F. Schweisguth, 1996 Subcellular localization of Suppressor of Hairless in Drosophila sense organ cells during Notch signalling. Development 122: 1673–1682.

Golic, K. G., and S. Lindquist, 1989 The FLP recombinase of yeast catalyzes site-specific recombination in the Drosophila genome. Cell 59: 499–509.

Harris, R. E., M. Pargett, C. Sutcliffe, D. Umulis, and H. L. Ashe, 2011 Brat promotes stem cell differentiation via control of a bistable switch that restricts BMP signaling. Dev. Cell 20: 72–83.

Herold, N., C. L. Will, E. Wolf, B. Kastner, H. Urlaub *et al.*, 2009 Conservation of the protein composition and electron microscopy structure of *Drosophila melanogaster* and human spliceosomal complexes. Mol. Cell. Biol. 29: 281–301.

Ji, X., Y. Zhou, S. Pandit, J. Huang, H. Li *et al.*, 2013 SR proteins collaborate with 7SK and promoter-associated nascent RNA to release paused polymerase. Cell 153: 855–868.

Johnston, L. A., D. A. Prober, B. A. Edgar, R. N. Eisenman, and P. Gallant, 1999 Drosophila myc regulates cellular growth during development. Cell 98: 779–790.

Juge, F., C. Fernando, W. Fic, and J. Tazi, 2010 The SR protein B52/SRp55 is required for DNA topoisomerase I recruitment to chromatin, mRNA release and transcription shutdown. PLoS Genet. 6: e1001124.

Jumaa, H., G. Wei, and P. J. Nielsen, 1999 Blastocyst formation is blocked in mouse embryos lacking the splicing factor SRp20. Curr. Biol. 9: 899–902.

Karni, R., E. de Stanchina, S. W. Lowe, R. Sinha, D. Mu *et al.*, 2007 The gene encoding the splicing factor SF2/ASF is a proto-oncogene. Nat. Struct. Mol. Biol. 14: 185–193.

Lin, S., and X.-D. Fu, 2007 SR proteins and related factors in alternative splicing. Adv. Exp. Med. Biol. 623: 107–122.

Luo, Z., C. Lin, and A. Shilatifard, 2012a The super elongation complex (SEC) family in transcriptional control. Nat. Rev. Mol. Cell Biol. 13: 543–547.

Luo, Z., C. Lin, E. Guest, A. S. Garrett, N. Mohaghegh *et al.*, 2012b The Super elongation complex family of RNA polymerase II elongation factors: gene target specificity and transcriptional output. Mol. Cell. Biol. 32: 2608–2617.

Michelotti, E. F., G. A. Michelotti, A. I. Aronsohn, and D. Levens, 1996 Heterogeneous nuclear ribonucleoprotein K is a transcription factor. Mol. Cell. Biol. 16: 2350–2360.

Muse, G. W., D. A. Gilchrist, S. Nechaev, R. Shah, J. S. Parker *et al.*, 2007 RNA polymerase is poised for activation across the genome. Nat. Genet. 39: 1507–1511.

Nascimento, E. M., C. L. Cox, S. MacArthur, S. Hussain, M. Trotter *et al.*, 2011 The opposing transcriptional functions of Sin3a and c-Myc are required to maintain tissue homeostasis. Nat. Cell Biol. 13: 1395–1405.

Oskarsson, T., and A. Trumpp, 2005 The Myc trilogy: lord of RNA polymerases. Nat. Cell Biol. 7: 215–217.

Pignoni, F., and S. L. Zipursky, 1997 Induction of Drosophila eye development by decapentaplegic. Development 124: 271–278.

Ring, H. Z., and J. T. Lis, 1994 The SR protein B52/SRp55 is essential for Drosophila development. Mol. Cell. Biol. 14: 7499–7506.

Sen, S., H. Jumaa, and N. J. G. Webster, 2013 Splicing factor SRSF3 is crucial for hepatocyte differentiation and metabolic function. Nat. Commun. 4: 1336.

Shi, H., B. E. Hoffman, and J. T. Lis, 1999 RNA aptamers as effective protein antagonists in a multicellular organism. Proc. Natl. Acad. Sci. USA 96: 10033–10038.

Sonoda, J., and R. P. Wharton, 2001 Drosophila brain tumor is a translational repressor. Genes Dev. 15: 762–773.

Sun, S., Z. Zhang, R. Sinha, R. Karni, and A. R. Krainer, 2010 SF2/ASF autoregulation involves multiple layers of post-transcriptional and translational control. Nat. Struct. Mol. Biol. 17: 306–312.

Tomonaga, T., and D. Levens, 1995 Heterogeneous nuclear ribonucleoprotein K is a DNA-binding transactivator. J. Biol. Chem. 270: 4875–4881.

Tripathi, V., J. D. Ellis, Z. Shen, D. Y. Song, Q. Pan *et al.*, 2010 The nuclear-retained noncoding RNA MALAT1 regulates alternative splicing by modulating SR splicing factor phosphorylation. Mol. Cell 39: 925–938.

Walters, A. D., A. Bommakanti, and O. Cohen-Fix, 2012 Shaping the nucleus: factors and forces. J. Cell. Biochem. 113: 2813–2821.

Wang, H. Y., X. Xu, J. H. Ding, J. R. Bermingham, and X. D. Fu, 2001 SC35 plays a role in T cell development and alternative splicing of CD45. Mol. Cell 7: 331–342.

Wittwer, F., A. van der Straten, K. Keleman, B. J. Dickson, and E. Hafen, 2001 Lilliputian: an AF4/FMR2-related protein that controls cell identity and cell growth. Development 128: 791–800.

Wu, H., S. Sun, K. Tu, Y. Gao, B. Xie *et al.*, 2010 A splicing-independent function of SF2/ASF in microRNA processing. Mol. Cell 38: 67–77.

Xu, X., and X.-D. Fu, 2005 Conditional knockout mice to study alternative splicing in vivo. Methods 37: 387–392.

Xu, X., D. Yang, J.-H. Ding, W. Wang, P.-H. Chu *et al.*, 2005 ASF/SF2-regulated CaMKIIdelta alternative splicing temporally reprograms excitation-contraction coupling in cardiac muscle. Cell 120: 59–72.

Zhong, X.-Y., P. Wang, J. Han, M. G. Rosenfeld, and X.-D. Fu, 2009 SR proteins in vertical integration of gene expression from transcription to RNA processing to translation. Mol. Cell 35: 1–10.

Zhou, Z., and X.-D. Fu, 2013 Regulation of splicing by SR proteins and SR protein-specific kinases. Chromosoma 122: 191–207.

Communicating editor: M. Wolfner

GENETICS

Supporting Information
http://www.genetics.org/lookup/suppl/doi:10.1534/genetics.115.174391/-/DC1

A Role for the Serine/Arginine-Rich (SR) Protein B52/SRSF6 in Cell Growth and Myc Expression in *Drosophila*

Céline Fernando, Agnès Audibert, Françoise Simon, Jamal Tazi, and François Juge

DOI: 10.1534/genetics.115.174391

Figure S1
Fernando et al.

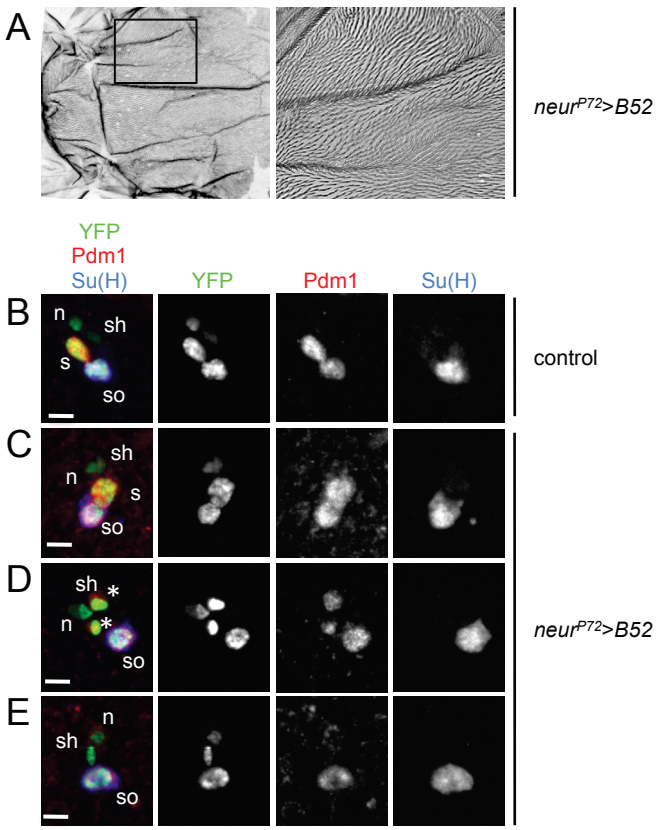

Figure S1. Effect of B52 overexpression with the *neur^{P72}-GAL4* driver on bristle cell lineage development. (A) External phenotype of *neur^{P72}>B52* individuals. Overexpression of B52 under the control of *neur^{P72}-GAL4* is lethal in embryos. We therefore introduced a transgene ubiquitously expressing a thermosensitive version of the GAL4 inhibitor GAL80 (GAL80^{ts}). Embryonic and larval development was carried out at permissive temperature, and pupae were shifted to restrictive temperature to release GAL4 activity during pupal development. This gives rise to pharat adults displaying an almost total loss of thoracic bristles. Right panel is a higher-magnification image of the field indicated by the box in the left panel. (B-E) Cellular clusters in microchaetes from control (B) and *neur^{P72}>B52* (C-E) pupae at 36 h APF. Sensory cells were identified with YFP (green in merged images). pIIa daughter cells (shaft and socket cells) are identified by Pdm1 immunoreactivity (red in merged images). Of these, only socket cells express Su(H) protein (blue in merged images). Following B52 overexpression, three types of cluster are observed, clusters with four cells (C), clusters in which the shaft cells are dying (star in D), and a cluster without the shaft cell (E). The absence of shaft and socket cells in the external cuticle indicates that socket cells die after 36 h APF. sh, sheath cell; n, neuron; s, shaft cell; so, socket cell. (B-E) Scale bars, 2 µm.

Figure S2
Fernando et al.

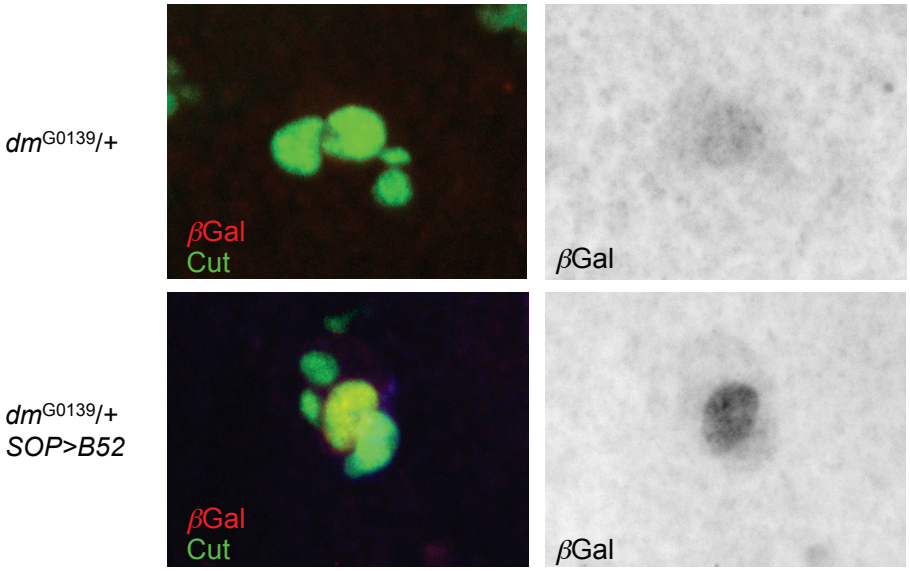

Figure S2. B52 overexpression enhances expression of the *lacZ* enhancer trap in *dm*^{G0139}.
Anti-*b*Galactosidase staining of macrochaete lineages in heterozygous females *dm*^{G0139}/+ overexpressing B52 (bottom panel) or not (top panel). Bristle lineage is detected by Cut antibody.

Figure S3
Fernando et al.

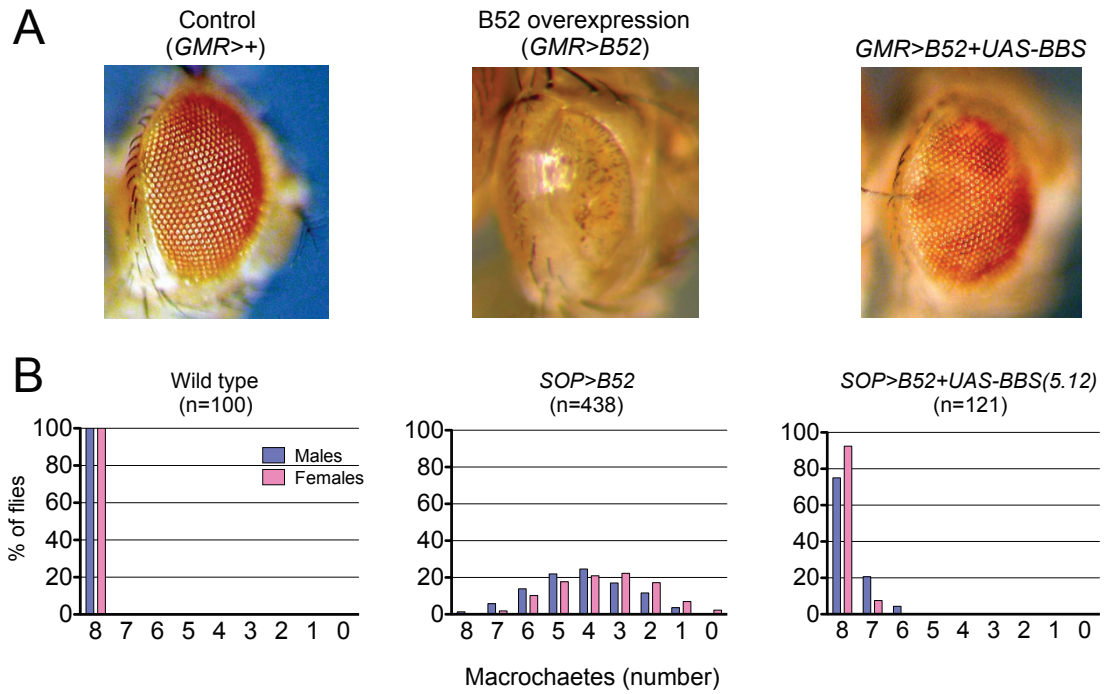

Figure S3. Rescue of the phenotypes induced by B52 overexpression in the eye (A) or bristles (B) by co-expression of the *UAS-BBS(5.12)* transgene.

Figure S4
Fernando et al.

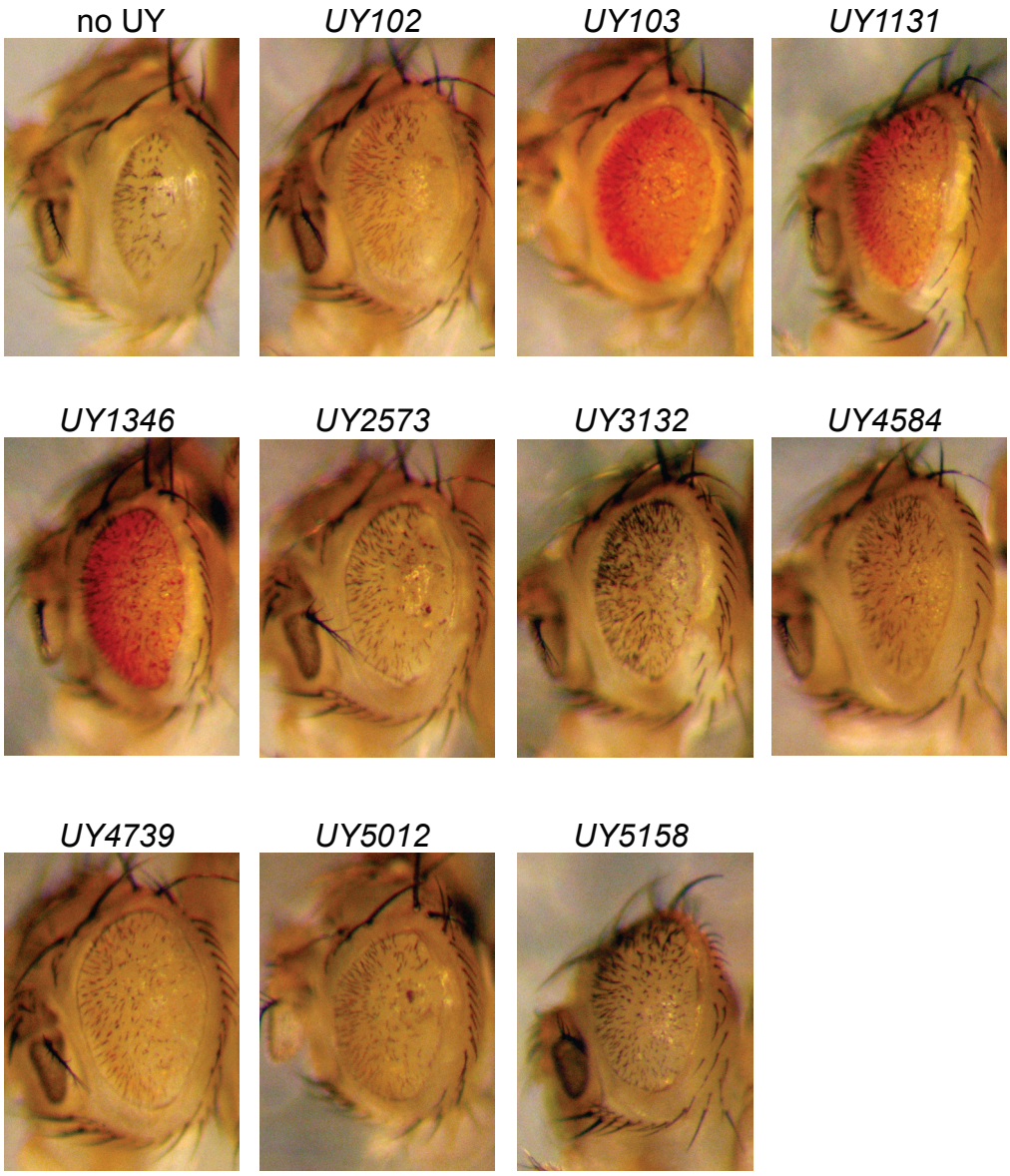

Figure S4. Rescue of the phenotype induced by B52 overexpression in the eye (*GMR-GAL4* driver) in the candidate lines identified by the screen.
The rescues obtained with the lines *UY3065* and *UY4508* are not shown because these lines were lost before completion of the screen.

Figure S5
Fernando et al.

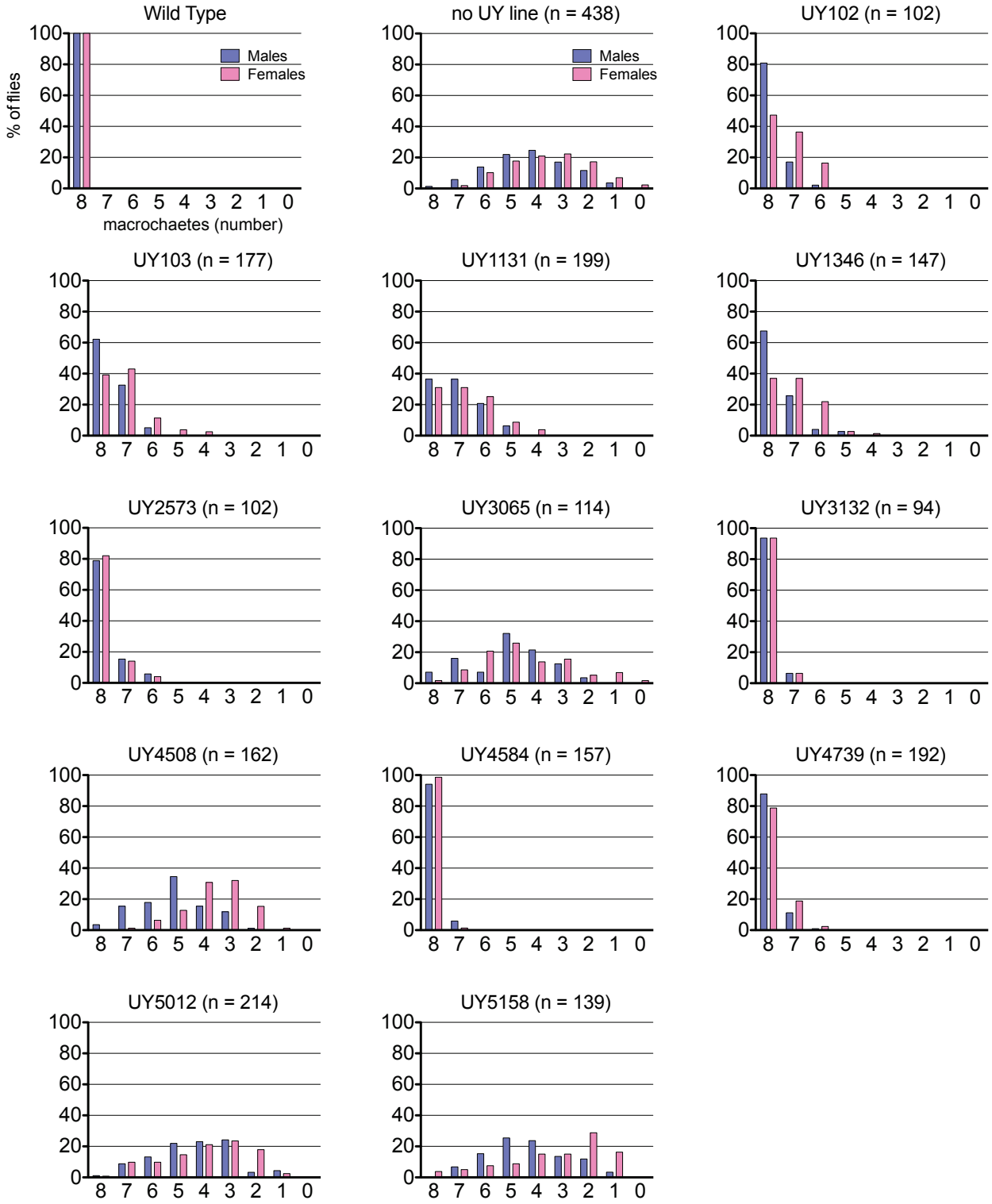

Figure S5. Rescue of the phenotype induced by B52 overexpression in the bristles (*SOP-GAL4* driver) in the candidate lines identified by the screen.
Histograms show the distribution of flies according to the number of macrochaetes. In the wild type, 100% of males and females have eight thoracic macrochaetes. The number of flies counted for each genotype is indicated in parentheses.

Figure S6
Fernando et al.

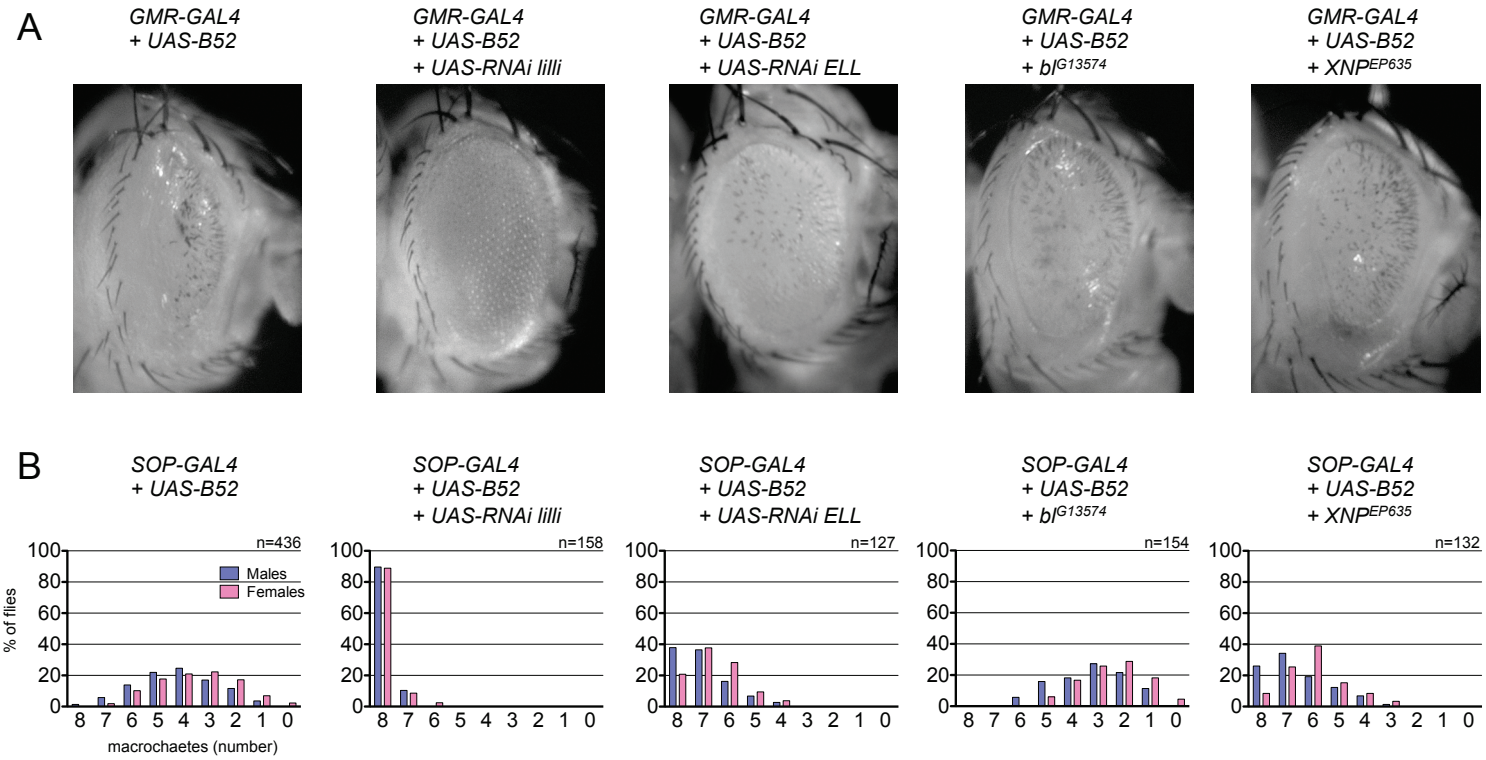

Figure S6. Rescue of the phenotypes induced by B52 overexpression by several candidate genes.
Rescue of the phenotypes induced by B52 overexpression in the eye (A) and bristles (B) by expression of an RNAi targeting *lilli*, an RNAi targeting ELL, or by forced expression of *bancal* (*bl*^{G13574}) or *XNP* (*EP635*). Histograms show the distribution of flies according to the number of macrochaetes. In the wild type, 100% of males and females have eight thoracic macrochaetes. The number of flies counted for each genotype is indicated at the top of each graph.

Figure S7
Fernando et al.

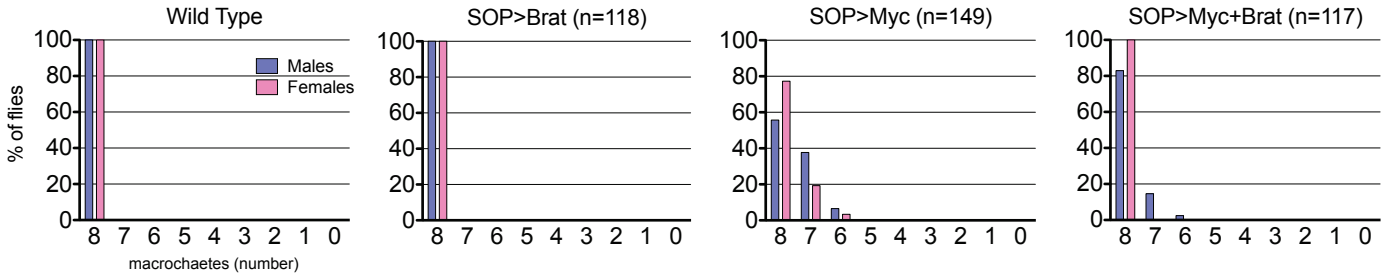

Figure S7. Brat antagonizes the effect of Myc overexpression in the bristle lineage.
Histograms show the distribution of flies according to the number of macrochaetes (dorso-central and scutellar macrochaetes). Overexpression of Brat under the control of the *SOP-Gal4* driver does not induce loss of macrochaetes, whereas overexpression of Myc in the same conditions induces a weak phenotype. Overexpression of Brat rescues the phenotype induced by Myc overexpression.
The number of flies counted for each genotype is indicated at the top of the graph.

Table S1. List of primers used in this study.

Primers pairs used for qRT-PCR	Primers pairs used for ChIP
B52 mRNA ATGCCGTCTATGAACTGAATG CCATTGAGAAGTTGGATGACAC	*dm* fragment 1 GTGGGGGATGTGGAAGTGTC CCGTCGTCTGCGTATTTGGC
myc mRNA GCCGAAAGCGACTGGAAAGC CGATGTTGCGGATCTCTGGC	*dm* fragment 2 AGAGAGGGTGTGATTTTTCGTCGCC CAGTTATGCTCACCGTAGGCCAGAA
myc pre-mRNA GCCGAAAGCGACTGGAAAGC CGATTTGTGCGGCCATGATC	*dm* fragment 3 GTCGCGTGTTCAGTTCACCG GCGGTTTTAAGTCGGCTCTTAGG
RP49 mRNA CACCAAGCACTTCATCCGCC TTCTTGGAGGAGACGCCGTGG	*dm* fragment 4 CCCTTTACCGCTCTGATCCGT CGATGTTGCGGATCTCTGGC
GAPDH mRNA TGAGGCGTTTGTGACTTCTG AACAGGGGGAATTTGTCCTC	*dm* fragment 5 TCGTCGTGTTCGATGTGTCGC TCTTTGCCCCCGTCCATTTG
LacZ mRNA GGAAAGCTGGCTGGAGTGCG TCCGTGGGAACAAACGGCGG	*dm* fragment 6 GCTTCGATCCTTTCTTGACATTAAGCC ACCAAATCAAATCGCGCGGAA
	hsp70 +58 CAATTCAAACAAGCAAAGTGAACACA TGATTCACTTTAACTTGCACTTTA
	hsp70 +681 ATATCTGGGCGAGAGCATCACA GTAGCCTGGCGCTGGGAGTC
	hsp70 +1951 TGGACGAGGCTGACAAGAACT CCTTCTCGGCAGTGGTGTTG
	octβ3R TTGCTGTCTGGCGTAAATTG TCAGCGGAGTCCTTGAAGAT